Ratcheting fluid with geometric anisotropy

Benjamin Thiria, and Jun Zhang

Citation: Appl. Phys. Lett. **106**, 054106 (2015); doi: 10.1063/1.4906927
View online: https://doi.org/10.1063/1.4906927
View Table of Contents: http://aip.scitation.org/toc/apl/106/5
Published by the American Institute of Physics

Ratcheting fluid with geometric anisotropy

Benjamin Thiria[1,2] and Jun Zhang[1,3,a)]
[1]*Applied Mathematics Laboratory, Courant Institute of Mathematical Sciences, New York University, New York, New York 10012, USA*
[2]*Physique et Mécanique des Milieux Hétérogènes, ESPCI ParisTech, Paris, France*
[3]*Department of Physics, New York University, New York, New York 10003, USA and NYU-ECNU Institute of Mathematical Sciences at NYU-Shanghai, Shanghai 200122, China*

(Received 21 October 2014; accepted 14 January 2015; published online 3 February 2015)

We investigate a mechanism that effectively transports fluids using vibrational motion imposed onto fluid boundary with anisotropy. In our experiment, two asymmetric, sawtooth-like structures are placed facing each other and form a corrugated fluid channel. This channel is then forced to open and close periodically. Under reciprocal motion, fluid fills in the gap during the expansion phase of the channel and is then forced out during contraction. Since the fluid experiences different impedances when flowing in different directions, the stagnation point that separates flows of two directions changes within each driving period. As a result, fluid is transported unidirectionally. This ratcheting effect of fluid is demonstrated through our measurements and its working principle discussed in some detail. © *2015 AIP Publishing LLC*. [http://dx.doi.org/10.1063/1.4906927]

In order to transport fluid from one place to the other, many types of fluid pumps have been invented and they have become an indispensable part of our everyday life. The most commonly used fluid pumps are centrifugal and peristaltic pumps. The former often deals with large quantities of fluid and the latter carries more precisely controlled flux. Small amount of fluid can be transported using a ratcheting effect, where asymmetric geometries are often involved to induce the net motion of the fluid. For instance, it has been observed that shorebirds use asymmetric capillarity to move drops of water along their long beak in order to feed and drink.[1] Similar ratchets are found when surface tension plays an important role on structured surfaces.[2–4] At a much smaller length-scale, colloid particles are made to migrate within a sawtooth-like geometry when an electrical potential is switched on and off: particles are transported uni-directionally, thanks to the anisotropic boundary conditions and Brownian diffusion.[5–9] Other types of ratchets also exist in many applications[10] where spatial anisotropy and temporal cyclicality are needed.

In the current work, we study experimentally a simple pumping mechanism that transports fluid effectively, using only reciprocal motion and boundary asymmetry. We further characterize its pumping rate, dependency on some key parameters. Most importantly, we identify and examine its working principle as an alternative type of fluid pump. Further, we discuss its usefulness in future applications.

Our experimental setup consists of two chambers filled with water that are connected through a structured channel in between, as shown in Figs. 1(a) and 1(b). The channel is formed by two identical sawtooth-like panels that are made from acrylic plastic. Each panel has 12 teeth in the horizontal direction and height $d = 6.3$ mm over a length L of 7.6 cm and depth D of 4 cm. The facets of each tooth are made either vertical or 45° with respect to vertical (Fig. 1(c)). The bottom sawtooth is fixed to the base of the chamber. The top sawtooth, however, is rigidly connected to a wall that separates the two chambers. This wall may slide vertically, inside two fluid-tight grooves. An oscillatory mechanism of the Scotch-yoke type, not shown, drives the upper sawtooth to reciprocal motion. We control the frequency f and the peak-to-peak amplitude a of such motion, and the average gap between the sawtooth panels, G, which can be preset to any desired value ($G > a/2$). The pumping flux is measured by two overflow mechanisms installed on both side of the setup. They can also be used, by adjusting their relative height, Δh, to create a hydrostatic pressure difference. Our working fluid is water through out the quantitative measurements. For flow visualization within the corrugated tunnel, however, we use a refractive-index-matched fluid[11] to the acrylic. Seeded particles in the fluid are illuminated by a light sheet that is sent through the bottom, leaving strike patterns that reveals the flow structures inside the channel. It is observed that as the driving frequency or amplitude exceeds a threshold, as discussed later, the fluid starts to be pumped and the pumping direction *follows the direction of the teeth*. In Fig. 1, this direction is from left to the right. As Fig. 2 shows, at each gap G and amplitude a, the dependency of the fluid flux of the pumped fluids follows the same trends but does not overlap. Each curve shows a threshold over which the flux increases linearly with the forcing speed fa. If the forcing speed is rescaled, however, to faL/G, all data collapse onto a single curve, showing that the pumping speed Q/GD uniquely depends on the forcing speed.

Let us first understand this data collapse. In fact, the forcing speed faL/G is the *characteristic speed* of the fluid, filling and exiting the channel, at both ends of the tunnel. The reasoning is the following: over one period of forcing oscillation, the average size of the two openings is $2GD$. During the compression cycle of the forcing, the volume of the tunnel changes from $(G + a/2)LD$ to $(G - a/2)LD$, which is aLD. During this half cycle, which takes time $1/2f$, the incompressible fluid exists the tunnel. The characteristic speed is thus $(2f)(aLD)/2GD = faL/G$, same as that for the expansion cycle. Since usually we have $D \gg G$, the pumping

a)Author to whom correspondence should be addressed. Electronic address: jun@cims.nyu.edu

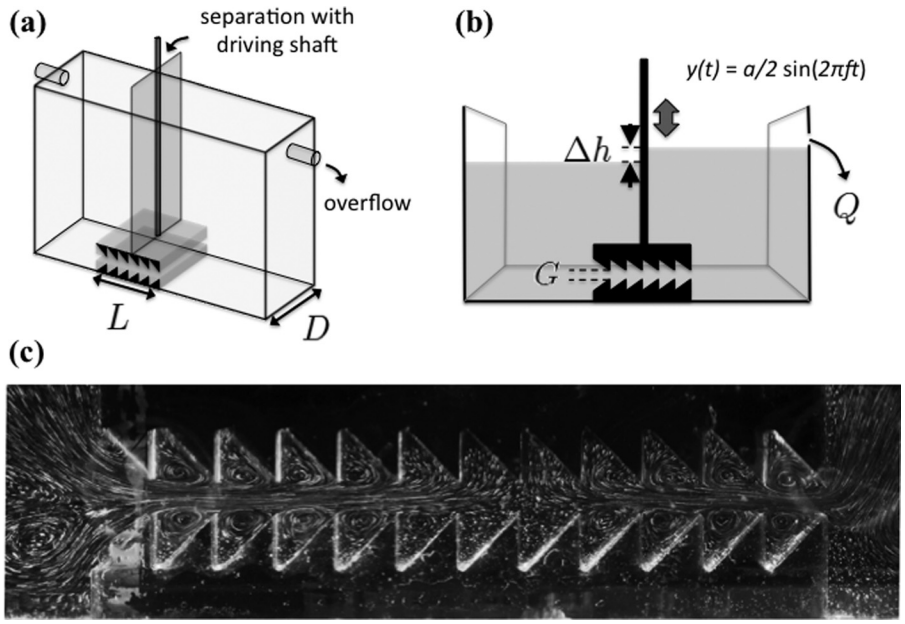

FIG. 1. Two schematic views of the experimental setup: (a) and (b) Two sawtooth-shaped panels were placed facing each other to form a channel, which connects the left and right chambers. The bottom sawtooth sits immobile in the fluid tank and the upper one is driven by a shaft, at a controlled frequency and amplitude. Once in action (switched on), fluid can be transported from the left to the right. The maximum pressure buildups and the maximum flow rates are measured separately. Flow visualization (c) within the gap, with polystyrene beads and a laser sheet, shows an instance as the upper saw-tooth moves up and the fluid fills the opening gap. Notice that the stagnation point between the two refilling flows is off the center and to the right.

mechanism is essentially two-dimensional, independent of D. The Reynolds number of the system, which is the characteristic ratio between initial force and viscose action, can be defined as $(faL/G) \times d \times (1/\nu) = faLd/G\nu$, where ν is the kinematic viscosity of the fluid. Since d and ν are constant in our experiment, the horizontal axis or the control parameter in Fig. 2(b) can be regarded as the Reynolds number. The data collapse seen in Fig. 2(b) suggests that the fluid-pumping mechanism is due to the finite Reynolds-number effect or the inertial effect. Here, the characteristic length involved in the Reynolds number expression is the depth d of the teeth, setting the size of the recirculation eddy next to each tooth. The choice of this expression (rather than scaling the Reynolds number on the channel gap G) will be justified later. Going back to Fig. 2, we find the threshold of the pumping mechanism to be around $\mathrm{Re} \sim 1800$. This large Reynolds number again implies that the pumping phenomenon is due to an inertia effect, which is only effective at high flow rates but will not work at the viscose limit. We note here that the value of the threshold Reynolds number is much higher than the one observed in works on similar periodically constricted geometry ($Re \sim 50$ see, for instance, Ref. 12). However, those previous works were conducted using an imposed steady flow that makes the comparison difficult with our time-dependent system in terms of flow-transition. Nevertheless, the inertial flow separation mechanisms described above, which will be seen to be at the base of the pumping phenomenon, are similar.

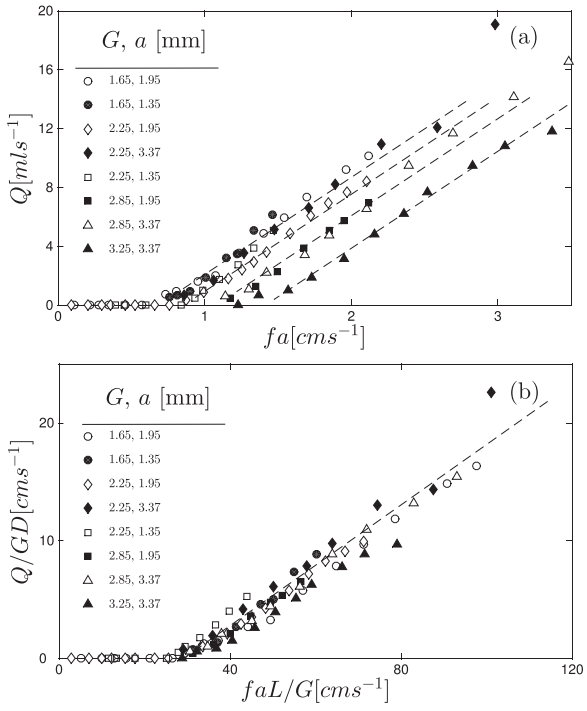

FIG. 2. Fluid pumping rates are plotted against dimensional driving speeds in the vertical direction (when $\Delta h = 0$). Top: Experimental data are shown in eight groups of channel gap G and forcing amplitude a against the driving frequency f. As a function of the characteristic driving speed fa, the ratchet starts to pump fluid when fa exceeds a threshold, which depends on G, a, and f. Inset: a table of symbols that are grouped with G and a. Bottom: Normalized pumping speeds Q/GD verses the normalized forcing speed faL/G. The same data shown on the top now collapse onto a common curve.

Now we investigate the working principle of this fluid ratchet. In order to reveal the effect of the geometric asymmetry on the fluid, we first measure the flow flux when the tunnel is held steady ($a = 0$) and at an imposed pressure drop $\rho g \Delta h$, where ρ and g are the fluid density and g the acceleration of gravity, respectively. Not surprisingly, Fig. 3 shows the difference between two fluid fluxes: the flux goes with the teeth direction is higher than that against the teeth direction. This implies that the flow going from left to right experiences less impedance than that going from right to the left. In another word, it is easier to flow to the right and more difficult to flow to the left. This behavior is due to the inertial characteristic of the flow, coupled to the asymmetry of the teeth geometry. The vortices trapped within the teeth correspond to *lost* kinetic energy. Depending on the flow direction, the size and strength of the trapped eddies in the cavities may be different. The impedance difference observed in both directions can be defined by two drag coefficients $C_d^{\pm}$ characterizing a measure of flow losses in the channel, where the signs + and – refer to the flow, aligned

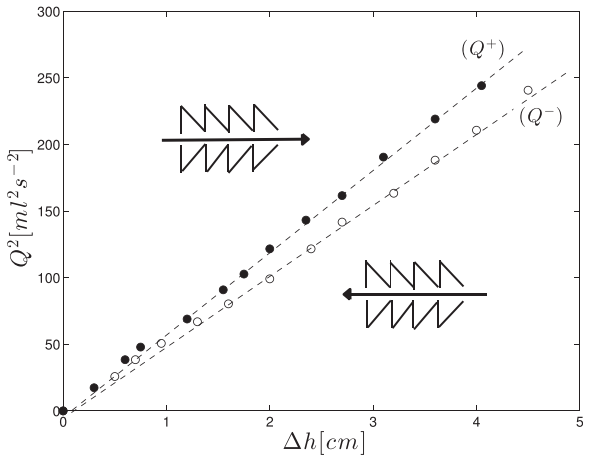

FIG. 3. Asymmetric flow rates measured at fixed gap $G = 2.25$ mm when the channel is stationary ($a = 0$). The upper curve shows a higher flux (Q^+), when the flow goes with the teeth direction, than that in the opposite direction (Q^-), at the same but opposite pressure head Δh. From these results, we found the drag coefficients in both directions $Cd^+ = 2.6$ and $Cd^- = 3.2$.

with and against the teeth/pumping direction, respectively. This method of characterization for channel flows has been extensively studied, for instance, in the context of heat transfer, for estimating the energy losses in longitudinal vortices (see Ref. 13). Because of the asymmetric teeth design, favoring flow going from left to right, we have $C_d^+ < C_d^-$. Measurements for our corrugated channel gave the following drag coefficients in both directions $Cd^+ = 2.6$ and $Cd^- = 3.2$.[14] We note that in this steady flow experiment, the threshold Reynolds number is about $Re \sim 80$, which is consistent with Ref. 12. When the forcing is activated, the consequence of above effect is shown in Fig. 4. During the opening phase, fluid has to fill up the opening tunnel and two opposing flows meet somewhere in the middle of the tunnel. Since the two flows have different impedances, they two meet at a point somewhere to the right side (top panel). During the closing phase, fluid exits the tunnel and the

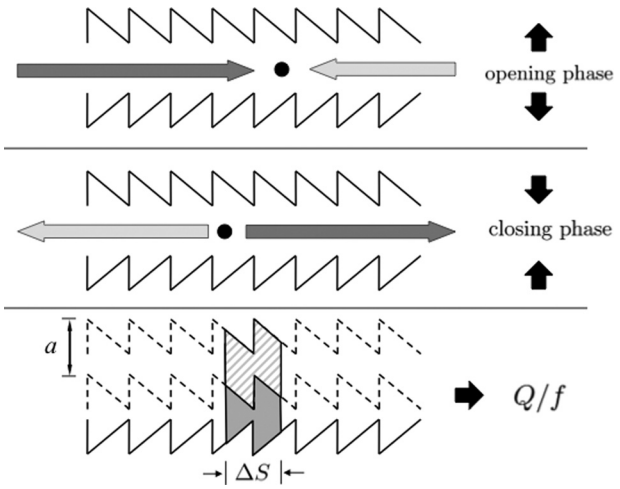

FIG. 4. Schematic of the pumping mechanism. Top: During the opening cycle, two opposing flows fill the tunnel and meet somewhere in the middle but biased to the right. This is due to the smaller impedance for the rightward flow. Middle: During the closing cycle, the fluid flows out from the center of the channel but the separation is biased to the left. Bottom: The shift ΔS thus defines a volume of fluid, shown as the dashed area multiplied by the tunnel depth D, which is transported to the right, following the direction of the teeth.

separation point of the two opposing flows shifts somewhere to the left at a distance ΔS away (middle panel). As a result, a volume of fluid, shown as the dashed area multiplied by the tunnel depth D, is transported to the right, following the direction of the teeth.

Flow visualization of the meeting position between the two flows confirms this mechanism. Shown in Fig. 5, the shift of the meeting position can be identified and measured by the strike-pattern of the particles. Below frequency $f = 2$ Hz, which is below the critical Reynolds number, the meeting position stays put, at the axis of symmetry of the system. Above a threshold, $\Delta S \neq 0$, the fluid starts to be pumped. Quantity $\Delta V = aD\Delta S$ is the volume of the fluid been pumped from left to right per cycle and the flux is $afD\Delta S$. Indeed, plot $f\Delta S$ vs. f does show the same characteristics as shown in Fig. 2(b). Unlike a conventional channel flow, trapped eddies between the teeth, as shown in Fig. 1(c), offer a slip conditions for the main flow occurring in the middle of the channel. This slip condition discards the role of viscosity in dissipating energy due to shear stresses in the velocity profile. Hence, the amount of kinetic energy provided by the pressure drop is mainly divided into the kinetic energy of the main channel flow and the kinetic energy *lost* in creating the eddies. Thus, for a smooth channel of length L and gap G with slip conditions, the total kinetic energy is $E_0 = \rho U_0^2 GLD/2$, where U_0 is the velocity at the entrance of the channel (set by the water height in a free fall configuration). In our corrugated channel, this energy becomes $\rho\bar{U}^2 GLD/2 + \rho C_d^{\pm}\bar{U}^2 Nd^2 D/2$, where $\bar{U}$ indicates the mean velocity in the channel, and N is the number of teeth on each panel. This simple partition gives an expression for the mean velocity $\bar{U}$

$$\bar{U}^{\pm} = \frac{U_0}{(1+\gamma^{\pm})^{1/2}}, \tag{1}$$

where $\gamma^{\pm} = \frac{Nd^2}{GL} C_d^{\pm} = \frac{d}{G} C_d^{\pm}$ are geometrical parameters involving the drag coefficients C_d^+ and C_d^- in both directions and the ratio between the volume of fluid within the teeth and the channel. Physically, the drag coefficients express the asymmetry of the teeth design, whereas the ratio $\frac{d}{G}$ plays the role of an amplification factor. When the system is under periodical forcing, the time $\tau = 1/2f$ for two particles of fluid coming from the opposite sides of the channel to meet inside at a location x is $\tau = 1/2f = x/\bar{U}^+ = (L-x)/\bar{U}^-$. It is then easy to estimate the shift ΔS, which reads

$$\Delta S = 2x - L = L\left(\frac{2}{\left(\frac{1+\gamma^+}{1+\gamma^-}\right)^{1/2} + 1} - 1\right). \tag{2}$$

It is worth to note that the shift ΔS is constant (for a given G), which is in agreement with the observations of Fig. 5 and only depends on the difference between drag coefficients, or impedance (i.e., depends only on the teeth design). Of course, this explanation only holds for cases that are far from the viscous limit, at high Reynolds numbers. The pumping rate of our ratchet also depends sensitively on the gap G. Shown in Fig. 6, the maximum pressure head can be achieved, where $Q = 0$ decreases monotonically with increased G. The

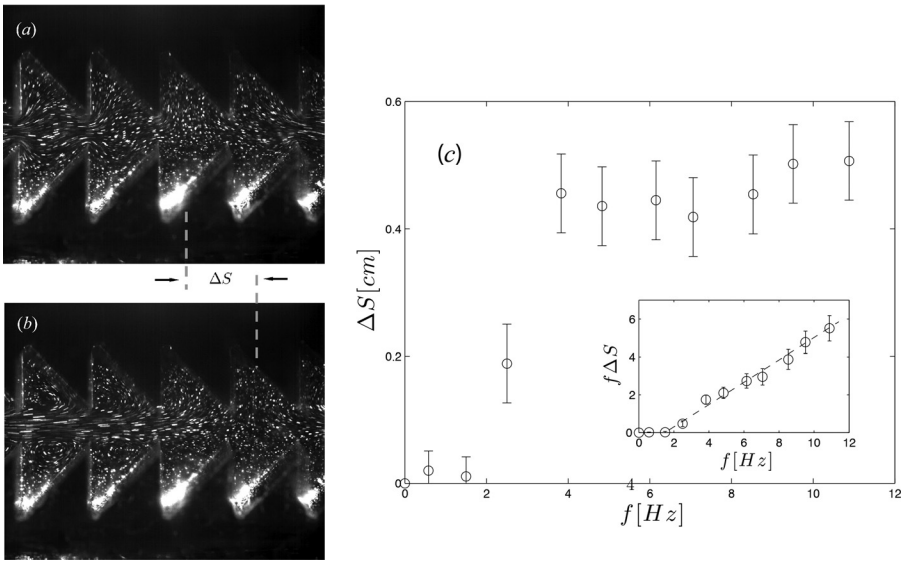

FIG. 5. Flow visualization of the central portion of the oscillating channel, during its closing phase (a) and opening phase (b). Two opposing flows meet at different locations as seen from the tracing particles, indicated by the dashed lines. The shift ΔS is measured and plotted in (c) against the forcing frequency. Above a finite frequency, the shift ΔS stays essentially constant. As shown in the inset, quantity $f\Delta S$ shows the same trend as the pumping flux, as in Fig. 2(b). Here $G = 2.25$ mm and $a = 1.95$ cm. (Multimedia view) [URL: http://dx.doi.org/10.1063/1.4906927.1]

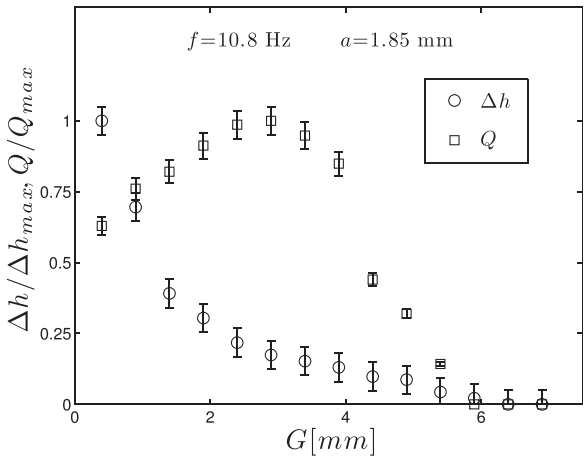

FIG. 6. As a function of the gap G between the two sawtooth, maximum pressure head achieved by the ratchet pump decreases monotonically (circles). The maximum pumping flux (squares), however, changes with G in a nonlinear fashion.

pumping flux Q, however, is a non-monotonic function of G. It climbs to a maximum value at a moderate value of G and then decreases as G is further increased. For the flux dependency on G, the increasing stage may be understood by considering the confinement effect due to the small volume involved in that regime (as we expect $Q \to 0$ when $G \to 0$). It has a finite starting value of flux due to the fact that G is finite ($G > a/2$). The decreasing phase of Q, however, comes from to the fact that the mean flux is not only a function of the driving speed fa but also of the ratio between the volumes of fluid within the teeth and the channel through the geometrical function $(1+\gamma^+)/(1+\gamma^-)$. This is an increasing function of G that asymptotically approaches to unity, which will lead to $\Delta S = 0$ as shown in Eq. (2). This result is consistent with the observation from our experiment (Fig. 6). We envision that the ratchet pump discussed in this work might invite some practical applications. Unwanted and sometimes dangerous vibration can be found near heavy machineries. Such vibration can be damped and even be used as ratchet pumps discussed here. Say, for example, coolant fluid can be pumped and circulated around such machines, which may improve the longevity of the machines and leads to better working environment. Some biological systems could have benefited from this ratcheting effect to pump body fluids around. Its usefulness will be the subject of our future studies.

We thank Sunny Jung and Bin Liu for their assistance and helpful discussions. We also thank the support from NSF (DMS-0652775, MRI-0821520 and DMR-0820341) and DOE (DE-FG02-88ER25053).

[1]M. Prakash, D. Quéré, and J. W. M. Bush, Science **320**, 931 (2008).
[2]H. Linke, B. J. Alemán, L. D. Melling, M. J. Taormina, M. J. Francis, C. C. Dow-Hygelund, V. Narayanan, R. P. Taylor, and A. Stout, Phys. Rev. Lett. **96**, 154502 (2006).
[3]G. Lagubeau, M. Le Merrer, C. Clanet, and D. Quéré, Nat. Phys. **7**, 395 (2011).
[4]A. Buguin, L. Talini, and P. Silberzan, Appl. Phys. A **75**, 207 (2002).
[5]M. O. Magnasco, Phys. Rev. Lett. **71**, 1477 (1993).
[6]J. Prost, J.-F. Chauwin, L. Peliti, and A. Ajdari, Phys. Rev. Lett. **72**, 2652 (1994).
[7]J. Rousselet, L. Salome, A. Ajdari, and J. Prost, Nature **370**, 446 (1994).
[8]L. Faucheux, L. Bourdieu, P. Kaplan, and A. Libchaber, Phys. Rev. Lett. **74**, 1504 (1995).
[9]C. Kettner, P. Hanggi, and F. Muller, Phys. Rev. E **61**, 312 (2000).
[10]C. Marquet, A. Buguin, L. Talini, and P. Silberzan, Phys. Rev. Lett. **88**, 168301 (2002).
[11]R. Budwig, Exp. Fluids **17**, 350 (1994).
[12]A. Lahbabi and H.-C. Chang, Chem. Eng. Sci. **41**, 2487 (1986).
[13]M. Fiebig, P. Kallweit, M. Mitra, and S. Tiggelbeck, Exp. Therm. Fluid Sci. **4**, 103 (1991).
[14]The drag coefficients have been estimated by fitting the experimental results of Fig. 3 using the energy balance giving an estimation of the mean velocity $\bar{U}^{\pm} = U_0/(1+\gamma\pm)^{1/2}$ in the channel (Eq. (1)) and by considering a free fall expression for the velocity $U_0 = \sqrt{2g\Delta h}$. The drag coefficients in both directions then write: $C_d^{\pm} = \sqrt{2g\Delta h}GD/(1+d/G)Q^{\pm}$. For the particular tooth design studied here, we found $Cd^+ = 2.6$ and $Cd^- = 3.2$.